From confined spinons to emergent fermions: Observation of elementary magnetic excitations in a transverse-field Ising chain

Zhe Wang,[1,*] Jianda Wu,[2,†] Shenglong Xu,[2] Wang Yang,[2] Congjun Wu,[2] Anup Kumar Bera,[3,‡] A. T. M. Nazmul Islam,[3] Bella Lake,[3,4] Dmytro Kamenskyi,[5] Papori Gogoi,[5] Hans Engelkamp,[5] Nanlin Wang,[6,7] Joachim Deisenhofer,[1] and Alois Loidl[1]

[1]*Experimental Physics V, Center for Electronic Correlations and Magnetism, Institute of Physics, University of Augsburg, 86135 Augsburg, Germany*

[2]*Department of Physics, University of California, San Diego, California 92093, USA*

[3]*Helmholtz-Zentrum Berlin für Materialien und Energie, 14109 Berlin, Germany*

[4]*Institut für Festkörperphysik, Technische Universität Berlin, 10623 Berlin, Germany*

[5]*High Field Magnet Laboratory (HFML-EMFL), Radboud University, 6525 ED Nijmegen, The Netherlands*

[6]*International Center for Quantum Materials, School of Physics, Peking University, 100871 Beijing, China*

[7]*Collaborative Innovation Center of Quantum Matter, Beijing, China*

(Received 30 June 2016; published 16 September 2016)

We report on spectroscopy study of elementary magnetic excitations in an Ising-like antiferromagnetic chain compound $SrCo_2V_2O_8$ as a function of temperature and applied transverse magnetic field up to 25 T. An optical as well as an acoustic branch of confined spinons, the elementary excitations at zero field, are identified in the antiferromagnetic phase below the Néel temperature of 5 K and described by a one-dimensional Schrödinger equation. The confinement can be suppressed by an applied transverse field and a quantum disordered phase is induced at 7 T. In this disordered paramagnetic phase, we observe three emergent fermionic excitations with different transverse-field dependencies. The nature of these modes is clarified by studying spin dynamic structure factor of a 1D transverse-field Heisenberg-Ising (XXZ) model using the method of infinite time evolving block decimation. Our work reveals emergent quantum phenomena and provides a concrete system for testifying theoretical predications of one-dimension quantum spin models.

DOI: 10.1103/PhysRevB.94.125130

I. INTRODUCTION

Emergent states of matter in quantum magnets are characterized by their elementary excitations that can be induced and tuned in an external magnetic field. Due to enhanced quantum fluctuations and reduced dimensionality, the low-dimensional quantum magnets host very often exotic quantum states of matter [1–13]. Especially for the one-dimensional (1D) spin systems, realization of novel quantum spin states is not only of lively experimental interest [7–10,12,13] but also a constant focus of theoretical study [1,2,14–17], since quantitative description of the elementary excitations can be provided by rigorous theoretical approaches and precise comparisons between theoretical predictions and experimental results can be made [7–10,12,13,15].

In the 1D spin-1/2 systems, the elementary magnetic excitations are spinons with fractional spin quantum number $S = 1/2$ [18]. Confinement of the fractional spinon excitations can be even realized [9,10,19–22] as an analogy with quark confinement in particle physics [23]. The concept of spinon confinement is illustrated in [Figs. 1(a)–1(d)]. In a classical picture, the ground state of a spin-1/2 Ising antiferromagnetic chain corresponds to an antiparallel alignment of neighboring spins [Fig. 1(a)]. A single spin flip frustrates the intrachain exchange interactions J and creates two spinons, each with spin-1/2 [Fig. 1(b)]. Subsequent spin flips can lead to propagation of the spinons along the chain [Fig. 1(c)]. In the presence of weak interchain exchange interactions $J_\perp \ll J$ [Fig. 1(d)], a 3D Néel antiferromagnetic order can be stabilized at low temperature $T < T_N$ and the separation of spinons from each other is unfavorable due to the frustrated interchain couplings. Thus the two spinons feel a confining potential, increasing with the distance between them, and form quantized spinon bound states [Figs. 1(e) and 1(f)] [24,25]. Since the spinons are confined by the interchain couplings only in the antiferromagnetic phase, the magnetic phase transition can be thought as accompanied by a spinon confinement-deconfinement transition.

$SrCo_2V_2O_8$ is a representative realization of the paradigmatic 1D Heisenberg-Ising (XXZ) model. It crystallizes in the tetragonal structure with space group $I4_1cd$. Screw spin chains in $SrCo_2V_2O_8$ are constituted by edge-sharing CoO_6 octahedra and propagate along the crystallographic c axis [Fig. 1(g)] [26,27]. Each screw period consists of four Co^{2+} ions with effective spin $S = 1/2$, corresponding to the lattice constant c. The unit cell contains four screw chains with either left- or right-hand chirality [Fig. 1(h)]. Due to spin-orbit coupling and crystal field splitting, the Co^{2+} spins have an Ising-like anisotropy along the c axis [26,27]. The dominant exchange interaction J is antiferromagnetic and between the nearest-neighbor Co^{2+} spins in the chain. The interchain coupling $J_\perp$ is much smaller and dominated by exchange between the nearest-neighbor Co^{2+} ions in the ab plane that are from the neighboring chains with the same chirality [Fig. 1(h)]. At $T_N = 5$ K a long-range Néel-type antiferromagnetic order along the chain is stabilized [Fig. 1(g)] [26–29].

*zhe.wang@physik.uni-augsburg.de

†jdwu@physics.ucsd.edu

‡Present address: Solid State Physics Division, Bhabha Atomic Research Centre, Mumbai 400085, India.

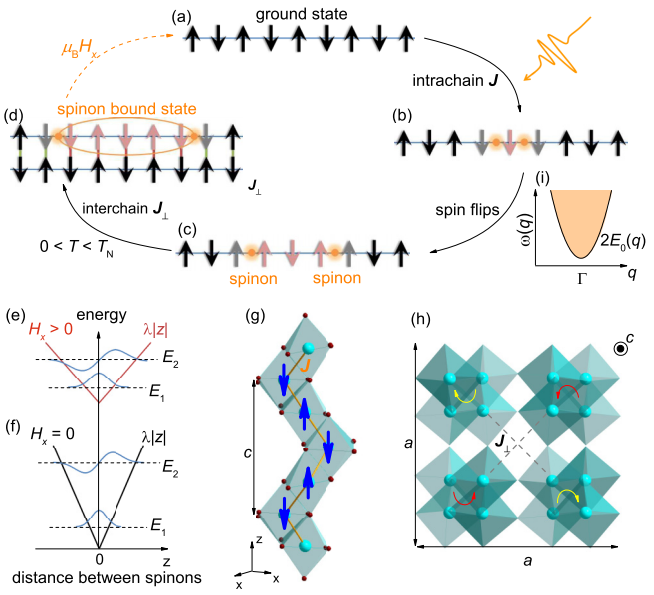

FIG. 1. (a) Ground state of an antiferromagnetic Ising chain with antiparallel alignment of neighboring spins. (b) A single spin-flip excitation composed of two spinons (orange dots). (c) Spinons can propagate along the chain by subsequent spin flips due to xy components of the exchange interactions. (d) Two spinons form a spinon bound state due to the frustration of interchain exchange $J_\perp$. (e), (f) Potential energy increases linearly with distance between spinons $V(z) = \lambda|z|$ with $\lambda = 2J_\perp\langle S_z\rangle^2/c$ and c is the lattice constant along the chain direction, covering four spin sites in $SrCo_2V_2O_8$ [see (g), (h)]. The two lowest-lying spinon bound states with energies E_1 and E_2 are schematically shown for zero and finite transverse fields H_x with $\lambda(H_x = 0) > \lambda(H_x > 0)$. (g) Screw chain of edge-shared CoO_6 octahedra propagating along the crystallographic c axis in $SrCo_2V_2O_8$ with antiferromagnetic order of Co^{2+} spins along the c direction stabilized below the Néel temperature $T < T_N$. (h) Viewing of left- and right-handed screw chains along the c direction. The dominant interchain exchange $J_\perp$ is between the nearest-neighbor Co ions in the ab plane, which are from the chains with the same chirality. $J_\perp > 0$ is antiferromagnetic. (i) Parabolic dispersion relation of the energy threshold $2E_0$ in the reciprocal space close to the Γ point ($q = 0$) [24,25].

Below T_N confinement of spinons is characterized by a series of quantized spinon bound states [Fig. 1(f)] [22], which with spin $S = +1$ or -1 can be split in longitudinal magnetic field and exhibit linear field dependence [20,22]. By applying a transverse magnetic field, the Néel temperature can be reduced according to the magnetic susceptibility measurements [26,27,30–32]. At 2 K, a phase transition from the Néel antiferromagnetic (AFM) phase to a disordered paramagnetic (PM) phase is induced by a transverse field of 7 T [26,27].

The reduction of Néel temperature suggests that the applied transverse magnetic field competes with the weak interchain couplings, and thus reduces the confining effects. This motivates us to utilize a transverse field to tune the spinon confinement. By continuously changing the transverse field, the confinement is expected to be suppressed with deconfined spinons observed.

Here we perform terahertz spectroscopy on the low-energy spin excitations in the 1D Ising-like antiferromagnetic-chain $SrCo_2V_2O_8$ as a function of transverse magnetic field, supplemented by studying spin dynamics of the corresponding 1D transverse-field XXZ model using the rigorous method of infinite time evolving block decimation (iTEBD). In zero field and below T_N, confinement of spinons of optical branch as well as of acoustic branch is observed and identified. Both the optical and the acoustic series of confined spinons can be described by a 1D Schrödinger equation with linear confining potential. In small transverse fields, where the system remains antiferromagnetically ordered, the confining effects are found to be reduced: the confining potential becomes shallower with increasing field and the higher energy spinon bound states tend to collapse on the lowest level. At the transverse-field-induced order-disorder transition, we observe collapse of the quantized confined-spinon levels. Above this transition, the low-energy spin excitations in $SrCo_2V_2O_8$ are not deconfined spinons, but characterized by emergent fermions of the 1D transverse-field Ising class. We successfully identify the observed emergent fermions and their field dependencies by performing theoretical study of the 1D spin-1/2 XXZ model using the iTEBD method.

II. EXPERIMENTAL DETAILS AND THEORETICAL METHOD

High-quality single crystals of $SrCo_2V_2O_8$ were grown using the floating-zone method and charactized by x-ray diffraction, neutron diffraction, and magnetization measurements [26]. Single crystals for the optical study were oriented using Laue diffraction and cut perpendicular to the tetragonal a axis with a typical surface of 4×4 mm^2 and a thickness of 1 mm. High-field optical measurements were performed in the High Field Magnet Laboratory in Nijmegen. A Michelson interferometer with mercury lamp was used to generate electromagnetic waves in the terahertz frequency range which were detected by a silicon bolometer cooled at 1.6 K. The sample transmission spectrum was measured in the spectral range of 1.2–10 meV (0.3–2.5 THz) at magnetic fields up to 25 T. Magnetic fields were applied perpendicular to the crystallographic ac plane and parallel to the propagation direction of the electromagnetic wave (Faraday configuration).

Standard infinite time evolving block decimation (iTEBD) method [33,34] was used to study spin dynamics of the 1D XXZ antiferromagnetic model in a transverse field. This method has been applied to other 1D systems [33,35] and turned out to be efficient to study 1D spin dynamics. Similar to the method of density matrix renormalization group, the iTEBD method assumes that the ground state (GS) of the spin system can be expressed as a matrix product state [33,34]. The two-point correlation function

$$C(r,t) = \langle S_y(r,t)S_y(0,0) + S_z(r,t)S_z(0,0)\rangle_{GS} \qquad (1)$$

is calculated to compare with experimental results. The spin components S_y and S_z are coupled to the THz magnetic field and the applied external magnetic field is set along the x direction. The spin dynamic structure factor (DSF) can be

obtained via Fourier transformation

$$S^{yy+zz}(q,\omega) = \int_{-\infty}^{\infty} dr \int_{-\infty}^{\infty} dt\, C(r,t) e^{i(\omega t - qr)}, \qquad (2)$$

corresponding to the magnetic-dipole excitations observed in the optical measurements. In our calculation, the bond dimension is taken to be 40 and the discrete time step in the real time evolution is $0.02/J$. The maximal time difference $|t - t'|$ is set to $32/J$, and we apply the linear prediction method [35] to further improve the resolution.

III. EXPERIMENTAL RESULTS

A. Confinement of acoustic and optical spinons in zero field

A spin-flip excitation can be triggered by absorbing a photon, when the photon has the same energy as the two spinons created [Figs. 1(a) and 1(b)]. The resonance absorption of photons is manifested by a transmission minimum (or an absorption maximum) at the corresponding photon energy. After the creation, the two spinons can propagate along the chain [Fig. 1(c)]. In presence of an effective linear confining potential $\lambda|z|$, the two-spinon bound state $\varphi(z)$ as a function of the distance z between them can be described by the one-dimensional Schrödinger equation

$$-\frac{\hbar^2}{\mu}\frac{d^2\varphi}{dz^2} + \lambda|z|\varphi = (E - 2E_0)\varphi, \qquad (3)$$

with $\hbar$ the Planck constant, μ an effective mass, and $2E_0$ the energy threshold for creating two spinons. $\lambda = 2J_\perp\langle S_z\rangle^2/c$ is an effective description of the interchain exchange interaction $J_\perp$, with the lattice constant c. The solution of Eq. (3) is given by the linear dependence of E_i on ζ_i

$$E_i = 2E_0 + \zeta_i \lambda^{2/3}\left(\frac{\hbar^2}{\mu}\right)^{1/3}, \qquad (4)$$

where $i = 1,2,3,\ldots$ and ζ_i are given by the negative zeros of the Airy function $Ai(-\zeta_i) = 0$ [36].

Figure 2(a) shows the ratio of two transmission spectra of $SrCo_2V_2O_8$ that are measured above and below the Néel temperature $T_N = 5$ K. Spin excitations due to the magnetic phase transition are manifested by the peaks. One can see three groups of excitations that are denoted by α_i, β_i, and γ. Eigenenergies $E_{\alpha i}$ of the α_i series follow the linear dependence on ζ_i as given in Eq. (4) with $2E_0 = 0.68$ meV and $\lambda^{2/3}(\frac{\hbar^2}{\mu})^{1/3} = 0.38$ meV as shown in Fig. 2(b). This indicates that the α_i series is confined spinon excitations, which is consistent with previous study [22]. In the same representation [Fig. 2(b)], one can see that the β_i modes with higher eigenenergies $E_{\beta i}$ also follow a linear dependence and the linear fit is given by $2E_0 = 7.55$ meV and $\lambda^{2/3}(\frac{\hbar^2}{\mu})^{1/3} = 0.23$ meV. Thus the β_i modes can be identified as another branch of confined spinons. Compared to the α_i series, the β_i modes have higher energy threshold and larger effective mass, if the same confining potential is assumed for both branches.

It will be shown in the following that we are able to assign the α_i modes as confined spinons of acoustic branch and the β_i modes as of optical branch, in analogy with the concept of optical and acoustic phonons. In contrast, the mode γ at 7.72 meV does not exhibit a series of excitations with higher

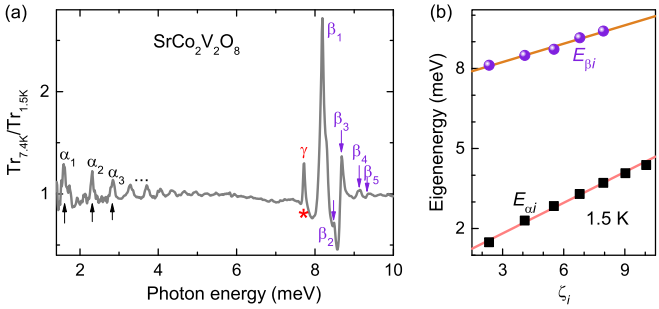

FIG. 2. (a) Ratio of transmission spectra that are measured at 7.4 K (above T_N) and at 1.5 K (below T_N). Two series of excitations α_i and β_i are observed and indicated by the arrows, corresponding to confined spinons of acoustic and optical branch, respectively. Another mode γ at 7.72 meV is marked by the star. (b) Eigenenergies $E_{\alpha i}$ and $E_{\beta i}$ of the modes α_i and β_i, respectively, as a function of ζ_i the negative zeros of the Airy function [36]. Linear fits according to the 1D Schrödinger equation are shown by the solid lines [see Eqs. (3) and (4)].

energies and thus not fit into the same scheme as the α_i and β_i modes. It is worth noting that the β_i modes are observed in the same energy range as the lower-lying optical phonon bands, making the higher energy levels difficult to resolve.

B. Tuning the spinon confinement in low transverse magnetic field

Figures 3(a) and 3(b) show transmission spectra of the acoustic α_i and optical β_i spinons of $SrCo_2V_2O_8$ as a function of applied transverse magnetic field along the crystallographic a axis ($H \parallel a$) up to 9 T. At zero field the series of

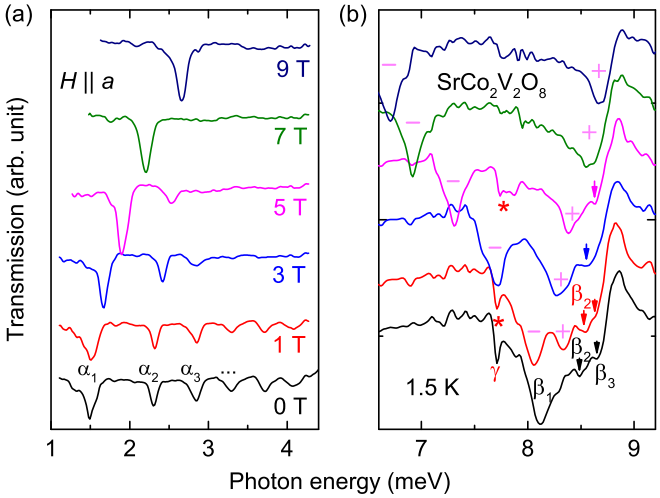

FIG. 3. Transmission spectra of (a) the acoustic α_i and (b) the optical β_i spinons in applied transverse magnetic fields along the crystallographic a axis ($H \parallel a$) up to 9 T. Series of absorption modes α_i can be observed at each field in (a). In (b) the zero-field mode β_1 splits into two modes in magnetic fields due to Zeeman interaction, as marked by the plus and minus signs. Below 7 T, shifting of the mode β_2 to higher energy with increasing fields is observed and indicated by the arrows. The γ mode at 7.72 meV, marked by the star, has almost field-independent eigenenergy below 7 T and is not resolvable at 7 T or above.

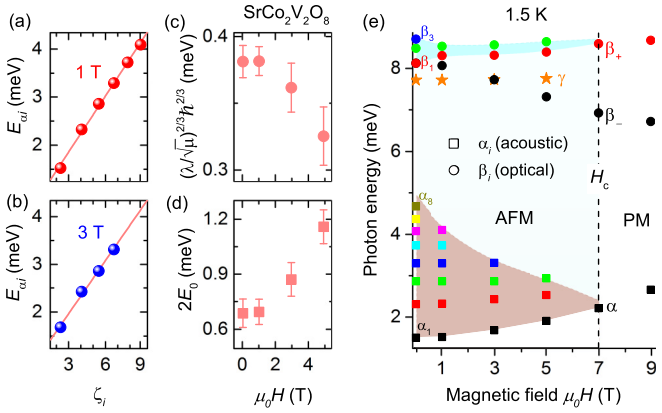

FIG. 4. (a), (b) Eigenenergies $E_{\alpha i}$ of the absorption modes α_i as a function of ζ_i for 1 T and for 3 T. The lines are linear fits according to the 1D Schrödinger equation with linear confining potential [Eqs. (3) and (4)]. (c), (d) The fitting parameters $\lambda^{2/3}(\frac{\hbar^2}{\mu})^{1/3}$ and $2E_0$ as functions of the transverse magnetic field. (e) Eigenenergies of the acoustic α_i, the optical β_i spinons, and the γ mode as functions of the magnetic field. At 7 T, the higher levels collapse to the lowest-level mode, α for the acoustic and β_+ for the optical spinons; the γ mode is suppressed; and only three modes α, β_+, and β_- remain. This indicates a field-induced phase transition from the antiferromagnetically (AFM) ordered to a paramagnetic (PM) quantum-disordered phase [26,27] at $H_c = 7$ T.

transmission minima, corresponding to confined acoustic and optical spinons, can be identified in agreement with the temperature-dependent measurements [Fig. 2(a)]. For the acoustic branch [Fig. 3(a)], a series of transmission minima for 1 T is observed at almost the same energies as for 0 T, while at 3 T the resolved modes are shifted to higher energies [see also Fig. 4(e)]. Interestingly, the dependence of the resonance energies E_i on ζ_i still follows the characteristic dependence at finite transverse fields, as shown in Figs. 4(a) and 4(b). This indicates that the spinon confinement is still a valid description of the spin dynamics in low transverse fields. The linear fit determines the parameters $\lambda^{2/3}(\frac{\hbar^2}{\mu})^{1/3} = 0.36$ meV and $2E_0 = 0.87$ meV for 3 T [Fig. 4(b)], where the former decreased while the latter significantly increased compared to the results at zero field. Thus, by applying a transverse magnetic field, one not only changes the energy threshold of the confined spinons, but also tunes the profile of the confining potential.

As shown in Figs. 4(c) and 4(d), the confining potential and threshold energy show a nonlinear decrease and increase, respectively, with increasing transverse field. This is different from the situation of small longitudinal fields along the Ising axis, where the threshold energy exhibits Zeeman-type linear dependence on field and the confining-potential profile is almost unchanged [20,22], since the $U(1)$ symmetry of the spin Hamiltonian is broken in the transverse field. The results in Figs. 4(c) and 4(d) suggest that the confining potential becomes shallower in the transverse field. In a shallower confining potential, as illustrated in Figs. 1(e) and 1(f), the difference between two neighboring spinon bound states reduces. When the difference becomes very small, the higher level cannot be distinguished experimentally. With increasing transverse field, the highest resolvable mode shifts to lower energy levels and, finally, when the second level (α_2) collapses onto the first one (α_1), the spinon hierarchy breaks down and the spinon confinement is completely suppressed.

As shown in Fig. 3(b), the zero-field optical mode β_1 splits into two in the transverse fields due to Zeeman interaction, one shifting up while the other shifting down, as marked by the plus and minus signs. The higher levels of confined optical spinons should be also split in the transverse field, since they belong to the same series. Due to strong phonon absorption at the same spectral range, fewer up-shifting confined modes of the optical branch can be resolved by the field-dependent measurements [marked by the arrows in Fig. 3(b)], while higher levels of the down-shifting modes are covered by the strong β_1 absorptions. Nevertheless, one can clearly observe some similar tuning behavior of the confined optical spinons as of the acoustic modes: the higher-level modes move towards the first level with increasing transverse field, although they all shift to higher energies with increasing fields; above 3 T the β_3 mode cannot be distinguished from the β_2 mode, and at 7 T only the main modes (β_+ and β_-) can be observed indicating the suppression of the spinon confinement.

In addition, the γ mode observed at 7.72 meV in zero field [Fig. 2(a)] shifts only slightly to higher energy and becomes broader with the increasing transverse fields. At 7 T, the γ mode is already suppressed. Although the origin of this mode remains unclear, it is natural to relate the γ mode to the 3D magnetic order because it is observed only below the magnetic phase transition.

The eigenenergies of the confined acoustic and optical spinons, and of the γ mode, are summarized in Fig. 4(e) as a function of the applied transverse magnetic field. Transverse-field tuning of the spinon confinement is obvious: starting from zero field, both the acoustic and optical spinons are confined due to the interchain couplings and exhibit clear hierarchy of the spinon bound states. With increasing field, the interchain couplings are effectively reduced and the higher-level bound states are shifted downwards until the second level collapses onto the first level at 7 T. The breakdown of the hierarchy, suggesting the suppression of the interchain couplings, is an evident signature of the field-induced phase transition [26,27].

C. Emergent fermions of 1D transverse-field Ising class

The above section documents the deconfining behavior of the confined spinons in a transverse magnetic field below the phase transition at $H_c = 7$ T. Above H_c in the quantum disordered phase, one would expect emergent elementary excitations that characterize spin state of the disordered phase. The characteristic excitations can be revealed by performing magneto-optic experiment in high magnetic fields.

A typical absorption-coefficient spectrum is shown in Fig. 5(a) for a transverse field of 11 T above the field-induced phase transition. One can observe three absorption maxima at 3.1, 6.4, and 8.8 meV, corresponding to the α, β_-, and β_+ modes, respectively. Their evolution with the transverse field is displayed in Fig. 5(c) by a contour plot of the absorption coefficient as a function of photon energy and transverse field, together with colored symbols highlighting their eigenenergies. The three modes α, β_-, and β_+ are the

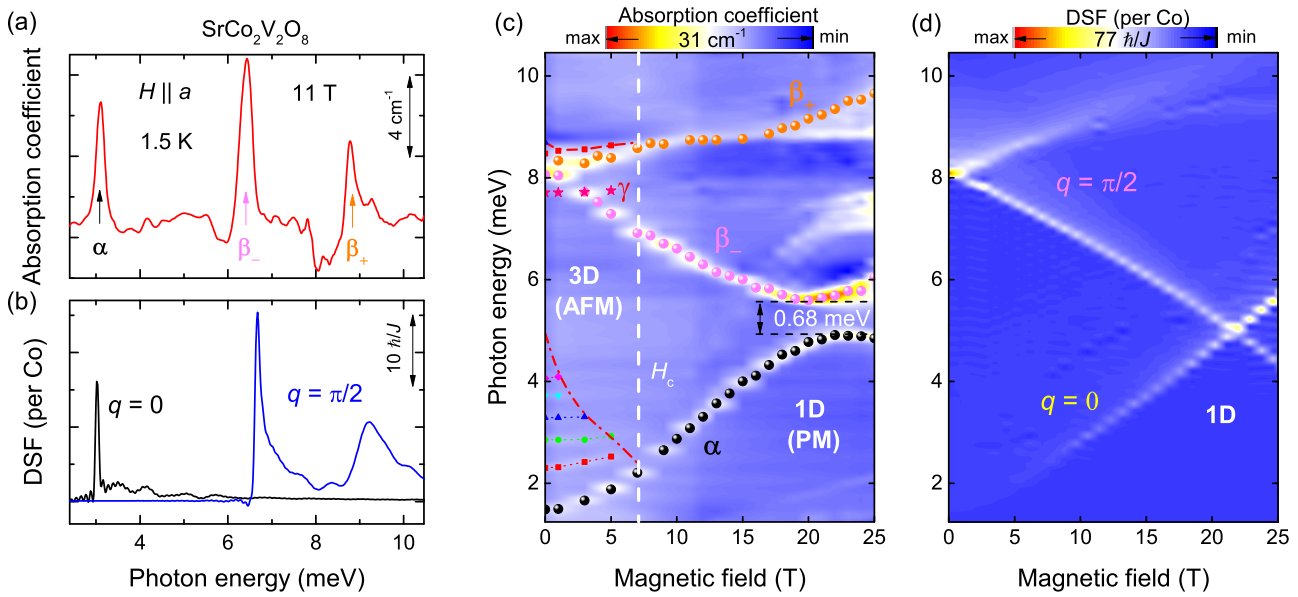

FIG. 5. (a) Absorption-coefficient spectrum measured in transverse magnetic field of 11 T at 1.5 K, exhibiting three spin excitation modes α, β_-, and β_+. The peak positions of the three modes are shown in (c) as a function of magnetic field (dots). (b) Spin dynamic structure factor (DSF) at $q = 0$ and $q = \pi/2$ as a function of energy in the corresponding transverse magnetic field, simulated by the iTEBD method [33,34] based on the 1D spin-1/2 XXZ model in Eq. (5). (c) Absorption coefficient and (d) DSF at $q = 0$ and $q = \pi/2$ as a function of photon energy and transverse magnetic field. The vertical dashed line at $H_c = 7$ T indicates the field-induced phase transition from the 3D antiferromagnetic (AFM) ordered to the 1D paramagnetic (PM) disordered phase [26,27]. In (c), the confined spinon levels E_i shown in Fig. 4(e) are also marked (symbols and dotted lines), and a hybridization gap of 0.68 meV is indicated. The calculated results in (b) and (d) are given with parameters $J = 3.55$ meV, $\Delta = 2.00$, and $g_x = 2.79$ (see text).

dominant excitations that can be unambiguously followed in higher fields.

The α mode, evolving from the lowest-lying confined spinon excitation α_1 [Figs. 3(a) and 4(e)], increases in energy with increasing fields. The β_- and β_+ modes correspond to the degenerate β_1 mode at zero field which is split in finite fields. At 22 T the α and β_- modes do not cross but form a small hybridization gap of 0.68 meV [Fig. 5(c)]. Above 22 T, the mode α shifts slightly downwards while the β_- mode shifts upwards.

IV. DISCUSSION

In order to understand origin of the observed modes in high fields and clarify the two branches of confined spinons, we use the standard iTEBD method [33,34] to study the spin dynamics of the spin-1/2 1D Heisenberg-Ising XXZ model, which describes the magnetic interactions of the cobalt spin chain. In a transverse magnetic field, the spin Hamiltonian is given by

$$J\sum_{\langle i,j\rangle}(S_{x,i}S_{x,j}+S_{y,i}S_{y,j}+\Delta S_{z,i}S_{z,j})-g_x\mu_B H_x\sum_i S_{x,i}, \tag{5}$$

where $\langle i,j\rangle$ denotes the nearest neighbors, J is the nearest-neighbor intrachain antiferromagnetic exchange interaction, and Δ refers to an Ising-like anisotropy [37,38]. The last term is the Zeeman interaction term with the transverse magnetic field H_x along the a axis, the Landé g factor, and the Bohr magneton μ_B.

The obtained spin dynamic structural factor (DSF) according to Eq. (2) is shown for the whole Brillouin zone at various transverse magnetic fields in Fig. 6. At zero field the known dispersion relation of spinons [10,39] is well reproduced in our calculations [Fig. 6(a)]. The dispersion relation is symmetric with respect to $q = \pi$. Two minima of the lower-energy boundary are degenerate and located at $q = 0$ and $q = \pi$, respectively. In a finite transverse field, the energy at $q = 0$ starts to increase and the corresponding minimum shifts to larger q values, while at $q = \pi$ the energy minimum is only slightly lowered. Moreover, a clear split of the dispersion relation occurs between $q = 0$ and $q = \pi$ and becomes more significant with the increasing transverse fields. These features of the dispersion relation characterize emergent fermions of the transverse-field Ising-like chain [40,41].

Terahertz spectroscopy is expected to probe the dispersion relation close to the Γ point ($q = 0$) in reciprocal space, since the wavelength of terahertz electromagnetic waves is much larger than the lattice constants of $SrCo_2V_2O_8$. To compare with the experimental results, in Fig. 5(d) the obtained DSF at $q = 0$ is shown as a function of energy and transverse magnetic field, which resembles the field dependence of the experimentally observed α mode. This indicates that the α fermionic excitations feature the spin dynamics at the Γ point and the corresponding confined spinons observed at zero field belong to an acoustic branch.

To reconcile the experimental results, the DSF at $q = \pi/2$ is also shown in Fig. 5(d) as a function of transverse field. An excitation mode close to 8 meV at zero field splits into two branches in the finite transverse fields, one increasing in energy while the other decreasing. Figure 5(b) shows the DSF

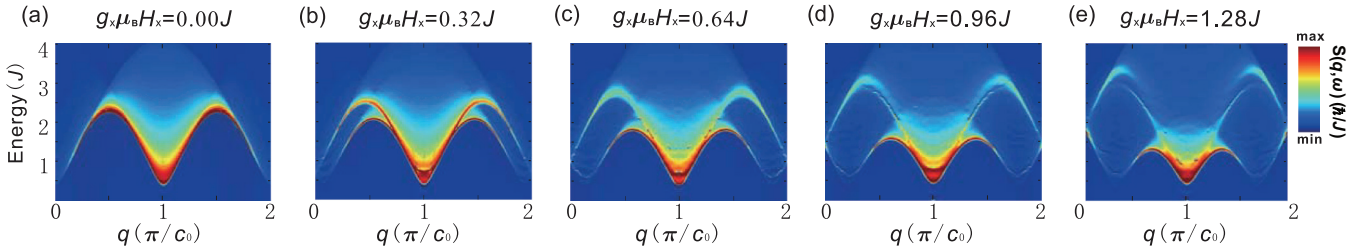

FIG. 6. (a)–(e) Spin dynamic structure factor $S(q,\omega)$ [Eq. (2)] in the reciprocal space $(0, 2\pi/c_0)$ calculated up to $4J$ for the 1D Heisenberg-Ising XXZ model Eq. (5) in various transverse magnetic fields $g_x\mu_B H_x$ of (a) 0, (b) 0.32, (c) 0.64, (d) 0.96, and (e) $1.28J$ by the iTEBD method [33,34]. c_0 is the natural lattice constant of the 1D XXZ model and J is the nearest-neighbor exchange interaction. The dynamic structure factor represents the dispersion relation of (a) spinons and (b)–(e) emergent fermions.

spectra of $q = 0$ and $q = \pi/2$ which agrees very well with the absorption-coefficient spectrum of 11 T in Fig. 5(a). The good agreement between experiment and theory is achieved with the parameters $J = 3.55$ meV, $g_x = 2.79$, and $\Delta = 2.00$. The g_x factor smaller than the longitudinal $g_\parallel = 5.5$ and the $\Delta > 1$ value reveals an Ising-like anisotropy [22]. The exchange interaction is quite larger than the value of $J = 2.8$ meV in $BaCo_2V_2O_8$ [20], while the anisotropy of the two systems is very close to each other.

These results indicate that the experimentally observed β_- and β_+ modes correspond to the emergent-fermion excitations at $q = \pi/2$ of the 1D transverse-field XXZ model, which are the low-energy spin excitations characteristic for the quantum disordered phase. It is also clarified that the β_i modes observed at zero field [Fig. 1(a)] can be assigned as confined spinons of optical branch, in analogy with the concept of optical phonons. At zero field the DSF at $q = \pi/2$ is much larger than that at $q = 0$. This explains the stronger absorption of the β_1 mode compared to the α_1 mode, as observed in Fig. 2(a).

The observation of the $q = \pi/2$ mode by optical spectroscopy indicates that the Brillouin zone is folded by a factor of four and translational invariance of the 1D XXZ model is broken due to the four spin sites per unit cell in $SrCo_2V_2O_8$ [Fig. 1(g)]. The zone-folding effect also explains the experimental observation of the hybridization gap at 22 T [Figs. 5(c)]. In the extended Brillouin zone the crossing of the acoustic α and optical β_- modes [Figs. 5(d)] is protected by the translational symmetry, since they are located at different q vectors. Due to the broken symmetry in the material, the transverse field can lead to nonzero off-diagonal elements of the interaction matrix, and thus mixes α and β_- states and opens the hybridization gap.

With further increasing transverse fields, our calculation suggests that the lower boundary at $q = \pi$ will be first gapless at 55 T, where a transverse-field Ising quantum critical point [40,41] is expected to emerge. At the quantum critical point, predicted dynamical features [16,42] are interesting to be testified in real materials.

V. SUMMARY

Using high-resolution terahertz spectroscopy, we have studied low-energy spin dynamics of the Ising-like antiferromagnetic chain $SrCo_2V_2O_8$ in transverse fields up to 25 T. According to the terahertz electrodynamic response, the transverse field-tuned spin dynamics is clarified and it can be categorized into three regimes:

(i) At zero field, the spin dynamics is characterized by confined spinons. We have identified confined spinons of an optical branch in addition to an acoustic branch. Both branches can be described by a 1D Schrödinger equation with linear confining potential. Compared to the acoustic one, the optical branch is found at higher energy with larger effective mass.

(ii) We have shown that the confinement of the optical and of the acoustic spinons can be tuned down by a small transverse field: the confining potential becomes shallower and the higher confinement levels are shifted closer to the lowest one. These properties can be viewed as deconfining behavior of the confined spinons, since the spinon series can be still described by the 1D Schrödinger equation and the small transverse field can be viewed as a perturbation.

(iii) We have also provided experimental evidence of the suppression of the spinon confinement by large transverse field, which is manifested by the collapse of the spinon hierarchy. This, however, does not result in deconfined spinons, but leads to the emergent-fermion excitations of the 1D transverse-field Ising class, because the transverse field is too strong to be treated as perturbation and even a phase transition from the antiferromagnetic to paramagnetic phase is induced. The evolution of emergent fermions in high transverse fields has been revealed by the terahertz spectroscopy and by studying low-energy spin dynamics of the 1D Ising-like XXZ model using the method of infinite time evolving block decimation. A quantum critical point of transverse-field Ising class is predicted to occur at 55 T yet to be testified.

ACKNOWLEDGMENTS

We would like to thank I. Affleck, S.-W. Cheong, B. Grenier, Zhangzhen He, T. Lorenz, A. Rosch, and S. Zvyagin for stimulating discussions. We acknowledge partial support by the Deutsche Forschungsgemeinschaft via the Transregional Research Collaboration TRR 80: From Electronic Correlations to Functionality (Augsburg - Munich - Stuttgart) and the Project DE 1762/2-1, and by the Chinesisch-Deutsches Zentrum für Wissenschaftsförderung. The high field experiments were supported by the HFML-RU/FOM, member of the European Magnetic Field Laboratory (EMFL). J.W., S.X., W.Y., and C.W. acknowledge the support by NSF DMR-1410375 and AFOSR FA9550-14-1-0168. J.W. acknowledges the hospitality of Rice

Center for Quantum Materials. C.W. acknowledges the supports from the President's Research Catalyst Awards No. CA-15-327861 from the University of California Office of the President, the National Natural Science Foundation of China (Grant No. 11328403), the CAS/SAFEA International Partnership Program for Creative Research Teams of China.

[1] T. Giamarchi, *Quantum Physics in One Dimension* (Oxford University Press, Oxford, 2004).
[2] V. Zapf, M. Jaime, and C. D. Batista, Bose-Einstein condensation in quantum magnets, Rev. Mod. Phys. **86**, 563 (2014).
[3] M. Punk, D. Chowdhury, and S. Sachdev, Topological excitations and the dynamic structure factor of spin liquids on the kagome lattice, Nat. Phys. **10**, 289 (2014).
[4] T. Han, J. S. Helton, S. Chu, D. G. Nocera, J. A. Rodriguez-Rivera, C. Broholm, and Y. S. Lee, Fractionalized excitations in the spin-liquid state of a kagome-lattice antiferromagnet, Nature (London) **492**, 406 (2012).
[5] B. Dalla Piazza, M. Mourigal, N. B. Christensen, G. J. Nilsen, P. Tregenna-Piggott, T. G. Perring, M. Enderle, D. F. McMorrow, D. A. Ivanov, and H. M. Rønnow, Fractional excitations in the square-lattice quantum antiferromagnet, Nat. Phys. **11**, 62 (2015).
[6] Z. Wang, D. L. Quintero-Castro, S. Zherlitsyn, S. Yasin, Y. Skourski, A. T. M. N. Islam, B. Lake, J. Deisenhofer, and A. Loidl, Field-Induced Magnonic Liquid in the 3D Spin-Dimerized Antiferromagnet $Sr_3Cr_2O_8$, Phys. Rev. Lett. **116**, 147201 (2016).
[7] B. Lake, D. A. Tennant, J.-S. Caux, T. Barthel, U. Schollwöck, S. E. Nagler, and C. D. Frost, Multispinon Continua at Zero and Finite Temperature in a Near-Ideal Heisenberg Chain, Phys. Rev. Lett. **111**, 137205 (2013).
[8] M. Mourigal, M. Enderle, A. Klöperpieper, J.-S. Caux, A. Stunault, and H. M. Rønnow, Fractional spinon excitations in the quantum Heisenberg antiferromagnetic chain, Nat. Phys. **9**, 435 (2013).
[9] R. Coldea, D. A. Tennant, E. M. Wheeler, E. Wawrzynska, D. Prabhakaran, M. Telling, K. Habicht, P. Smeibidl, and K. Kiefer, Quantum criticality in an Ising chain: Experimental evidence for emergent E8 symmetry, Science **327**, 177 (2010).
[10] B. Lake, A. M. Tsvelik, S. Notbohm, D. A. Tennant, T. G. Perring, M. Reehuis, Ch. Sekar, G. Krabbes, and B. Büchner, Confinement of fractional quantum number particles in a condensed-matter system, Nat. Phys. **6**, 50 (2010).
[11] J. P. Goff, D. A. Tennant, and S. E. Nagler, Exchange mixing and soliton dynamics in the quantum spin chain $CsCoCl_3$, Phys. Rev. B **52**, 15992 (1995).
[12] L. S. Wu, W. J. Gannon, I. A. Zaliznyak, A. M. Tsvelik, M. Brockmann, J.-S. Caux, M. S. Kim, Y. Qiu, J. R. D. Copley, G. Ehlers, A. Podlesnyak, and M. C. Aronson, Orbital-exchange and fractional quantum number excitations in an f-electron metal Yb_2Pt_2Pb, Science **352**, 1206 (2016).
[13] R. Toskovic, R. van den Berg, A. Spinelli, I. S. Eliens, B. van den Toorn, B. Bryant, J.-S. Caux, and A. F. Otte, Atomic spin-chain realization of a model for quantum criticality, Nat. Phys. **12**, 656 (2016).
[14] R. G. Pereira, J. Sirker, J.-S. Caux, R. Hagemans, J. M. Maillet, S. R. White, and I. Affleck, Dynamical Spin Structure Factor for the Anisotropic Spin-1/2 Heisenberg Chain, Phys. Rev. Lett. **96**, 257202 (2006).
[15] M. Kohno, Dynamically Dominant Excitations of String Solutions in the Spin-1/2 Antiferromagnetic Heisenberg Chain in a Magnetic Field, Phys. Rev. Lett. **102**, 037203 (2009).
[16] J. Wu, M. Kormos, and Q. Si, Finite-Temperature Spin Dynamics in a Perturbed Quantum Critical Ising Chain with an E_8 Symmetry, Phys. Rev. Lett. **113**, 247201 (2014).
[17] B. Bruognolo, A. Weichselbaum, J. von Delft, and M. Garst, Phys. Rev. B **94**, 085136 (2016).
[18] L. D. Faddeev and L. A. Takhtajan, What is the spin of a spin wave? Phys. Lett. A **85**, 375 (1981).
[19] C. M. Morris, R. Valdés Aguilar, A. Ghosh, S. M. Koohpayeh, J. Krizan, R. J. Cava, O. Tchernyshyov, T. M. McQueen, and N. P. Armitage, Hierarchy of Bound States in the One-Dimensional Ferromagnetic Ising Chain $CoNb_2O_6$ Investigated by High-resolution Time-Domain Terahertz Spectroscopy, Phys. Rev. Lett. **112**, 137403 (2014).
[20] S. Kimura, H. Yashiro, K. Okunishi, M. Hagiwara, Z. He, K. Kindo, T. Taniyama, and M. Itoh, Field-Induced Order-disorder Transition in Antiferromagnetic $BaCo_2V_2O_8$ Driven by a Softening of Spinon Excitation, Phys. Rev. Lett. **99**, 087602 (2007).
[21] B. Grenier, S. Petit, V. Simonet, E. Canévet, L.-P. Regnault, S. Raymond, B. Canals, C. Berthier, and P. Lejay, Longitudinal and Transverse Zeeman Ladders in the Ising-Like Chain Antiferromagnet $BaCo_2V_2O_8$, Phys. Rev. Lett. **114**, 017201 (2015).
[22] Z. Wang, M. Schmidt, A. K. Bera, A. T. M. N. Islam, B. Lake, A. Loidl, and J. Deisenhofer, Spinon confinement in the one-dimensional Ising-like antiferromagnet $SrCo_2V_2O_8$, Phys. Rev. B **91**, 140404(R) (2015).
[23] T. Muta, *Foundations of Quantum Chromodynamics* (World Scientific Publishing, Singapore, 1987).
[24] N. Ishimura and H. Shiba, Dynamical correlation functions of one-dimensional anisotropic Heisenberg model with spin 1/2. I. Ising-like antiferromagnets, Prog. Theor. Phys. **63**, 743 (1980).
[25] H. Shiba, Quantization of magnetic excitation continuum due to interchain coupling in nearly one-dimensional Ising-like antiferromagnets, Prog. Theor. Phys. **64**, 466 (1980).
[26] A. K. Bera, B. Lake, W.-D. Stein, and S. Zander, Magnetic correlations of the quasi-one-dimensional half-integer spin-chain antiferromagnets $SrM_2V_2O_8$ (M=Co, Mn), Phys. Rev. B **89**, 094402 (2014).
[27] Z. He, T. Taniyama, and M. Itoh, Antiferromagnetic-paramagnetic transitions in longitudinal and transverse magnetic fields in a $SrCo_2V_2O_8$ crystal, Phys. Rev. B **73**, 212406 (2006).
[28] E. Canévet, B. Grenier, M. Klanjšek, C. Berthier, M. Horvatić, V. Simonet, and P. Lejay, Field-induced magnetic behavior in quasi-one-dimensional Ising-like antiferromagnet $BaCo_2V_2O_8$: A single-crystal neutron diffraction study, Phys. Rev. B **87**, 054408 (2013).
[29] Y. Kawasaki, J. L. Gavilano, L. Keller, J. Schefer, N. B. Christensen, A. Amato, T. Ohno, Y. Kishimoto, Z. He, Y. Ueda, and M. Itoh, Magnetic structure and spin dynamics of the

quasi-one-dimensional spin-chain antiferromagnet $BaCo_2V_2O_8$, Phys. Rev. B **83**, 064421 (2011).

[30] S. K. Niesen, O. Breunig, S. Salm, M. Seher, M. Valldor, P. Warzanowski, and T. Lorenz, Substitution effects on the temperature versus magnetic field phase diagrams of the quasi-one-dimensional effective Ising spin-1/2 chain system $BaCo_2V_2O_8$, Phys. Rev. B **90**, 104419 (2014).

[31] S. K. Niesen, G. Kolland, M. Seher, O. Breunig, M. Valldor, M. Braden, B. Grenier, and T. Lorenz, Magnetic phase diagrams, domain switching, and quantum phase transition of the quasi-one-dimensional Ising-like antiferromagnet $BaCo_2V_2O_8$ Phys. Rev. B **87**, 224413 (2013).

[32] S. Kimura, K. Okunishi, M. Hagiwara, K. Kindo, Z. He, T. Taniyama, M. Itoh, K. Koyama, and K. Watanabe, Collapse of magnetic order of the quasi one-dimensional Ising-like antiferromagnet $BaCo_2V_2O_8$ in transverse fields, J. Phys. Soc. Jpn. **82**, 033706 (2013).

[33] G. Vidal, Classical Simulation of Infinite-Size Quantum Lattice Systems in One Spatial Dimension, Phys. Rev. Lett. **98**, 070201 (2007).

[34] R. Orús and G. Vidal, Infinite time-evolving block decimation algorithm beyond unitary evolution, Phys. Rev. B **78**, 155117 (2008).

[35] S. R. White and I. Affleck, Spectral function for the $S = 1$ Heisenberg antiferromagetic chain, Phys. Rev. B **77**, 134437 (2008).

[36] B. M. McCoy and T. T. Wu, Two-dimensional Ising field theory in a magnetic field: Breakup of the cut in the two-point function, Phys. Rev. D **18**, 1259 (1978).

[37] J. C. Bonner and M. E. Fisher, Linear magnetic chains with anisotropic coupling, Phys. Rev. **135**, A640 (1964).

[38] M. E. Lines, Magnetic properties of $CoCl_2$ and $NiCl_2$, Phys. Rev. **131**, 546 (1963).

[39] A. H. Bougourzi, M. Karbach, and G. Müller, Exact two-spinon dynamic structure factor of the one-dimensional $s = 1/2$ Heisenberg-Ising antiferromagnet, Phys. Rev. B **57**, 11429 (1998).

[40] D. V. Dmitriev, V. Ya. Krivnov, A. A. Ovchinnikov, and A. Langari, One-dimensional anisotropic Heisenberg model in the transverse magnetic field, J. Exp. Theor. Phys. **95**, 538 (2002).

[41] J.-S. Caux, F. H. L. Essler, and U. Löw, Dynamical structure factor of the anisotropic Heisenberg chain in a transverse field, Phys. Rev. B **68**, 134431 (2003).

[42] A. B. Zamolodchikov, Integrals of motion and s-matrix of the (scaled) $T = T_c$ Ising model with magnetic field, Int. J. Mod. Phys. A **04**, 4235 (1989).